Radiative transition processes between initial and final channels

Cheng Zhu,[1,2] Jian-Guo Wang,[3] Yi-Zhi Qu,[2] and Jia-Ming Li[1,2]
[1]*Center of Atomic and Molecular Sciences, Department of Physics, Tsinghua University, Beijing 100084, People's Republic of China*
[2]*Institute of Physics, Academia Sinica, P.O. Box 603, Beijing 100080, People's Republic of China*
[3]*Institute of Applied Physics and Computational Mathematics, P.O. Box 8009, Beijing 100088, People's Republic of China*
(Received 21 February 1997; revised manuscript received 7 August 1997)

Based on multichannel quantum-defect theory, a method to calculate and compile radiative transition processes for atoms (including highly ionized high-Z atoms) is proposed. Through defining the renormalized transition matrix elements from initial eigenchannels to final eigenchannels, the transition processes between infinitely many initial states and infinitely many final states can be treated conveniently. As illustrative examples, we study the alkali-metal atoms in detail. [S1050-2947(98)04903-8]

PACS number(s): 31.10.+z

I. INTRODUCTION

In recent years, with advances in many fields such as radio astronomy, radiation physics, and plasma physics, extensive quantities of atomic radiative transition data between excited states are needed. Although many works on these data have been published [1,2], they are still incomplete, since an excited atom involves infinitely many Rydberg states and adjacent continuum states. It is a formidable task to calculate all the transition processes individually. Even after we have obtained these data, it is still a problem to compile them efficiently. Thus it is an issue to find an efficient method to obtain and compile radiative transition data for excited atoms. In the past years, Bates and Damgaard have studied the ''bound-bound'' transitions [3], Burgess, Seaton, and Peach have studied the ''bound-free '' transitions [4,5], and Peach has studied the ''free-free '' transitions [6] for simple atomic systems (i.e., a single electron outside closed shells). In the present paper, the method we propose is based on multichannel quantum-defect theory (MQDT) and can be applied to any atoms or ions (including complex systems with high atomic number Z and high ionization degree q where a full relativistic treatment is required).

In the framework of MQDT, with a set of physical parameters $(\mu_\alpha, U_{i\alpha})$ which vary smoothly with the excitation energy, all the Rydberg states, autoionization states, and adjacent continuum states can be described in a unified manner [7–15]. According to MQDT, the energy eigenstate is a superposition of eigenchannels and the coefficients of the superposition can be calculated analytically by the boundary conditions at infinity. The transitions from a certain initial state to infinitely many final states can be treated as transitions from an initial state to final eigenchannels whose superpositions represent the final-energy eigenstates (i.e., final states) [11,12,16]. However, Burgess and Seaton's method can only be applied to one-channel problems [4]. Thus the calculation of the transition matrix elements from a specific initial state to any final state can be reduced to the calculation of the transition matrix elements from the specific initial state to final eigenchannels, which vary smoothly with the final eigenchannel energy. Similarly, the relevant infinitely many initial energy eigenstates (i.e., initial states) can be considered as superpositions of initial eigenchannels. Therefore the transitions from infinitely many initial states to infinitely many final states are reduced to transitions from initial eigenchannels to final eigenchannels. Here we present a method to calculate renormalized transition matrix elements from initial eigenchannels to final eigenchannels which vary smoothly with the initial and final eigenchannel energies. The initial and final eigenchannel wave functions can be obtained from first principles calculations by relativistic multichannel theory (RMCT) [17–20]. In earlier works which were only for one-channel problems [3–6], the concept of ''renormalized transition matrix element from initial eigenchannel to final eigenchannel'' has never been pointed out explicitly. In Bates and Damgaard's paper [3], the transition matrix elements calculated based on approximate analytical wave functions, which are accurate only for large radial distances, are expressed in the product form $F(n_l^*, l)I(n_{l-1}^*, n_l^*, l)$, where F is analytically known. For each l, I varies with two variables, n_{l-1}^* and n_l^*, in a large domain (i.e., $n_{l-1}^*, n_l^* \to \infty$) with smooth variations along the line of constant $n_{l-1}^* - n_l^*$. In our method, the renormalized transition matrix elements, which are calculated in an exact numerical manner without any analytical approximations, vary smoothly with two energy variables (initial and final energies, ϵ_i and ϵ_f). In order to obtain the transition matrix elements between infinitely many initial states and infinitely many final states, we need to perform interpolation on such renormalized transition matrix elements. Especially for transitions between infinitely many bound initial states and infinitely many bound final states, we only need to perform the interpolation in a very small domain (the lowest initial energy $\epsilon_{i0} \leqslant \epsilon_i < \epsilon_f \leqslant 0$). It can also be extended to the photoionization (bound-free) processes $(\epsilon_i < 0 \leqslant \epsilon_f)$ and the inverse-bremsstrahlung (free-free) transition processes $(0 < \epsilon_i < \epsilon_f)$. The transition matrix elements sometimes have nodal curves, on which the matrix elements equal zero. Such matrix elements near the nodal curves cannot be calculated analytically, since the main contributions come from smaller radial distances (also pointed out by Peach [5,6]). In this way, with only a few benchmark points, we can obtain any renormalized transition matrix elements from initial eigenchannels to final eigenchannels by interpolation instead of state-to-state calculations. Thus, the formidable radiative

transition data concerning infinitely many Rydberg states and adjacent continuum states can be calculated and compiled quite conveniently. As illustrative examples, we consider the alkali-metal atoms in the energy range around the first ionization threshold in detail; this is a one-eigenchannel problem in MQDT. For multichannel problems, the initial and final eigenchannel wave functions can be calculated by RMCT [17–20], and then, the renormalized transition matrix elements can be obtained similarly. Our calculated results show that the renormalized transition matrix elements of three kinds of transition processes, ''$s_{1/2}$-$p_{1/2}$,'' ''$p_{1/2}$-$d_{3/2}$,'' and ''$d_{3/2}$-$f_{5/2}$,'' for both K and Cs atoms form several smooth surfaces in the initial- and final-energy space, which represent all radiative transition processes between infinitely many initial and infinitely many final states.

II. THEORETICAL METHOD AND CALCULATIONAL RESULTS

Let us consider the transition processes of a general atomic system from an initial state ϵ_i to final states ϵ_f (including Rydberg states, autoionization states, and adjacent continuum states). According to MQDT [7–15], the final state wave function $|\epsilon_f\rangle$ can be written as the superposition of final eigenchannel wave functions,

$$|\epsilon_f\rangle=\sum_{\alpha_f}|\alpha_f\rangle A_{\alpha_f}^{\epsilon_f}, \tag{1}$$

where α_f is the index of final eigenchannels. The coefficients $A_{\alpha_f}^{\epsilon_f}$ and the eigenenergy of the final state ϵ_f can be calculated analytically through MQDT parameters. The transition matrix element from ϵ_i to ϵ_f can be written as

$$\langle\epsilon_i||D||\epsilon_f\rangle=\sum_{\alpha_f}\langle\epsilon_i||D||\alpha_f\rangle A_{\alpha_f}^{\epsilon_f}, \tag{2}$$

where D is the dipole transition operator and $\langle\epsilon_i||D||\alpha_f\rangle$ is the transition matrix element from initial state ϵ_i to final eigenchannel α_f. Therefore the calculation of the transition matrix element $\langle\epsilon_i||D||\epsilon_f\rangle$ from initial state to final state is reduced to the calculation of the transition matrix elements $\langle\epsilon_i||D||\alpha_f\rangle$ from initial state to final eigenchannels with energy normalization [8–15]. The final-energy normalized transition matrix elements vary smoothly with the final eigenchannel energy. With several benchmark points, the final-energy normalized transition matrix elements $\langle\epsilon_i||D||\alpha_f\rangle$ at any energy points can be obtained by interpolation, namely, the transition matrix elements from an initial state to final channels can be calculated conveniently by expression (2). Similarly, the relevant initial states ϵ_i (e.g., Rydberg states and autoionization states) can also be written as the superposition of initial eigenchannel wave functions

$$|\epsilon_i\rangle=\sum_{\alpha_i}|\alpha_i\rangle A_{\alpha_i}^{\epsilon_i}, \tag{3}$$

where α_i is the index of initial eigenchannels. The coefficients $A_{\alpha_i}^{\epsilon_i}$ and the eigenenergy of the initial state ϵ_i can be calculated analytically through MQDT parameters. From expressions (2) and (3), we get

$$\langle\epsilon_i||D||\epsilon_f\rangle=\sum_{\alpha_i}\sum_{\alpha_f}A_{\alpha_i}^{\epsilon_i}\langle\alpha_i||D||\alpha_f\rangle A_{\alpha_f}^{\epsilon_f}, \tag{4}$$

where $\langle\alpha_i||D||\alpha_f\rangle$ is the initial-final-energy normalized transition matrix element from initial eigenchannel α_i to final eigenchannel α_f. Therefore the calculation of the transition matrix element $\langle\epsilon_i||D||\epsilon_f\rangle$ from initial state to final state can be reduced to the calculation of the transition matrix element $\langle\alpha_i||D||\alpha_f\rangle$ from initial eigenchannel to final eigenchannel. Since $\langle\alpha_i||D||\alpha_f\rangle$ has the limiting behavior proportional to $\omega^{-5/3}$ when $\omega\to 0$ [21], we can define the renormalized transition matrix element from initial eigenchannel to final eigenchannel as

$$\langle\alpha_i||M||\alpha_f\rangle=\omega^{5/3}\langle\alpha_i||D||\alpha_f\rangle. \tag{5}$$

The renormalized transition matrix elements vary smoothly with initial and final eigenchannel energies, and form smooth surfaces in the energy space of initial and final eigenchannels. Only with several benchmark points can any renormalized transition matrix element on the surface be obtained by interpolation. Therefore any transition matrix element $\langle\epsilon_i||D||\epsilon_f\rangle$ from initial state to final state and the corresponding absorption cross section can be calculated with much less calculational effort. For ''bound-bound'' transitions, the absorption cross section is written as [22]

$$\sigma=\frac{\pi e^2 h}{mc}f_{\epsilon_i,\epsilon_f}L, \tag{6}$$

where L is the profile factor such that $\int L\,d\epsilon=1$. $f_{\epsilon_i,\epsilon_f}$ is the oscillator strength,

$$f_{\epsilon_i,\epsilon_f}=\frac{2\omega}{3g_{\epsilon_i}}|\langle\epsilon_i||D||\epsilon_f\rangle|^2, \tag{7}$$

where ω is the photon energy and g_{ϵ_i} is the degeneracy of initial state. For ''bound-free'' transitions, the absorption cross section is written as [22]

$$\sigma=\frac{\pi e^2 h}{mc}\ \frac{df_{\epsilon_i,\epsilon_f}}{d\epsilon}, \tag{8}$$

where $(df_{\epsilon_i,\epsilon_f}/d\epsilon)$ is the oscillator strength density,

$$\frac{df_{\epsilon_i,\epsilon_f}}{d\epsilon}=\frac{2\omega}{3g_{\epsilon_i}}|\langle\epsilon_i||D||\epsilon_f\rangle|^2. \tag{9}$$

As illustrative examples, we consider the alkali-metal atoms. Since the excitation energy of the core is relatively high, it is a one-channel problem in MQDT, and then there is only one term in the right side of expressions (2) and (4). The initial and final eigenchannel wave functions $|\alpha_i\rangle$, $|\alpha_f\rangle$ can be calculated adequately by the Dirac-Slater self-consistent field with local exchange approximation [23,24],

TABLE I. Comparison of orbital energy (in a.u.) for K.

State	Present work	Expt. [26]
$4s$	-0.1549	-0.1595
$5s$	-0.0623	-0.0624
$6s$	-0.0344	-0.0344
$7s$	-0.0216	-0.0216
$4p$	-0.0989	-0.1003
$5p$	-0.0468	-0.0469
$6p$	-0.0274	-0.0274
$7p$	-0.0179	-0.0179
$4d$	-0.0389	-0.0347
$5d$	-0.0246	-0.0220
$6d$	-0.0167	-0.0151
$7d$	-0.0120	-0.0110
$4f$	-0.0312	-0.0314
$5f$	-0.0200	-0.0201

in which the matrix elements calculated with length formula equal those calculated with velocity formula. The calculated orbital energies are in agreement with the experimental results within a few percent, and the agreement should be better for higher n orbitals as shown in Table I and Table II. The calculated transition wavelengths are also anticipated to be within a few percent. It may be adequate for most applications except for some special fine structure split transition lines, e.g., involving nf states of Cs with the abnormal inverse of fine structure ($nf_{7/2}<nf_{5/2}$) due to the difference of the relativistic nonlocal exchange interactions [25], which is very small anyway. Returning to the oscillator strength, the present calculated results are in fair agreement with the available tabulated values [26,27], as shown in Table III and

TABLE II. Comparison of orbital energy (in a.u.) for Cs.

State	Present work	Expt. [34]
$6s_{1/2}$	-0.1356	-0.1431
$7s_{1/2}$	-0.0579	-0.0586
$8s_{1/2}$	-0.0321	-0.0323
$6p_{1/2}$	-0.0891	-0.0921
$7p_{1/2}$	-0.0433	-0.0439
$8p_{1/2}$	-0.0258	-0.0259
$6p_{3/2}$	-0.0868	-0.0896
$7p_{3/2}$	-0.0425	-0.0431
$8p_{3/2}$	-0.0254	-0.0256
$6d_{3/2}$	-0.0419	-0.0401
$7d_{3/2}$	-0.0252	-0.0244
$8d_{3/2}$	-0.0169	-0.0164
$6d_{5/2}$	-0.0413	-0.0400
$7d_{5/2}$	-0.0250	-0.0243
$8d_{5/2}$	-0.0167	-0.0163
$6f_{5/2}$	-0.0139	-0.0140
$7f_{5/2}$	-0.0102	-0.0103
$8f_{5/2}$	-0.0078	-0.0079
$6f_{7/2}$	-0.0139	-0.0140
$7f_{7/2}$	-0.0102	-0.0103
$8f_{7/2}$	-0.0078	-0.0079

TABLE III. Comparison of oscillator strength for K.

State	Present work[a]	Wiese *et al.* [26][a]
$4s$-$4p_{1/2}$	3.47[−1]	3.39[−1](±25%)
$4s$-$5p_{1/2}$	3.32[−3]	3.05[−3](±25%)
$4s$-$6p_{1/2}$	4.23[−4]	2.99[−4](±25%)
$4s$-$7p_{1/2}$	1.15[−4]	7.1[−5](±25%)
$5s$-$5p_{1/2}$	5.01[−1]	5.0[−1](±50%)
$5s$-$6p_{1/2}$	9.55[−3]	1.1[−2](±50%)
$5s$-$7p_{1/2}$	1.68[−3]	2.0[−3](±50%)
$5p_{3/2}$-$6s$	3.22[−1]	3.2[−1](±50%)
$5p_{3/2}$-$7s$	2.67[−2]	2.7[−2](±50%)
$5p_{3/2}$-$8s$	8.57[−3]	8.7[−3](±50%)
$5p_{3/2}$-$4d_{3/2}$	7.34[−2]	1.2[−1](±50%)
. . .[b]	. . .	. . .

[a]The number $a[b]$ denotes $a\times10^{b}$.

[b]Since an excited atom involves infinitely many Rydberg states and adjacent continuum states, it is a formidable task to tabulate all the transition processes individually.

Table IV for K and Cs, respectively. When the renormalized transition matrix elements have nodal curves, in the vicinity of the nodal curves, the transition matrix elements cannot be described precisely by the Dirac-Slater approximation, but the absolute values of the transition matrix elements are very small anyway. Nevertheless, the present calculation with Dirac-Slater approximation will not affect the discussion of the general properties of the renormalized matrix elements between the initial eigenchannels and the final eigenchannels. The accuracy can be improved by the RMCT [17–20] or equivalent theoretical methods. For bound states ϵ_n, the corresponding eigenchannel wave function can be calculated according to the normalization per unit energy [16], namely, $|\alpha\rangle=|\epsilon_n\kappa_n\rangle(A_\alpha^{\epsilon_n})^{-1}$ with $(A_\alpha^{\epsilon_n})^{-2}=\nu_n^3/(q+1)^2$. Here ν_n is the effective principal quantum number, and q is the degree of ionization. For continuum states ϵ, the eigenchannel wave function $|\alpha\rangle=|\epsilon\kappa\rangle$ [corresponding to $(A_\alpha^{\epsilon})=1$]. Thus the renormalized transition matrix elements can be obtained. We have calculated the renormalized transition matrix elements of three kinds of transition processes, ''$s_{1/2}$-$p_{1/2}$,'' ''$p_{1/2}$-$d_{3/2}$,'' and ''$d_{3/2}$-$f_{5/2}$,'' for K and Cs, respectively, as shown in part (b) of Figs. 1–6 [in order to make a comparison, the corresponding final-energy normalized transition matrix elements $\langle\epsilon_i||D||\alpha_f\rangle$ are also shown, as in part (a)]. For the continuum-continuum transitions, we first calculate the rela-

TABLE IV. Comparison of oscillator strength for Cs.

State	Present work[a]	Moore [27][a]
$6s$-$6p$	1.15	1.04
$6s$-$7p$	2.14[−2]	1.48[−2]
$6s$-$8p$	4.26[−3]	2.0[−3]
. . .[b]	. . .	. . .

[a]The number $a[b]$ denotes $a\times10^{b}$.

[b]Since an excited atom involves infinitely many Rydberg states and adjacent continuum states, it is a formidable task to tabulate all the transition processes individually.

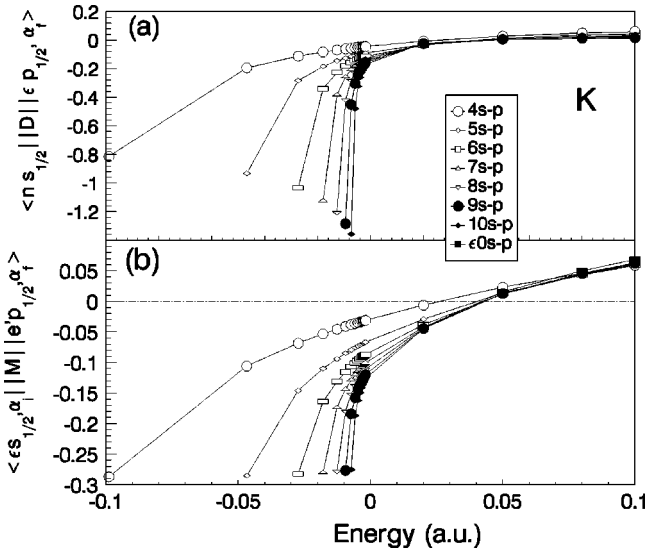

FIG. 1. (a) Final-energy normalized matrix elements $\langle ns_{1/2}||D||\epsilon p_{1/2},\alpha_f\rangle$, (b) renormalized matrix elements $\langle \epsilon s_{1/2},\alpha_i||M||\epsilon' p_{1/2},\alpha_f\rangle$ for K, here $\epsilon 0=0.01$ a.u.

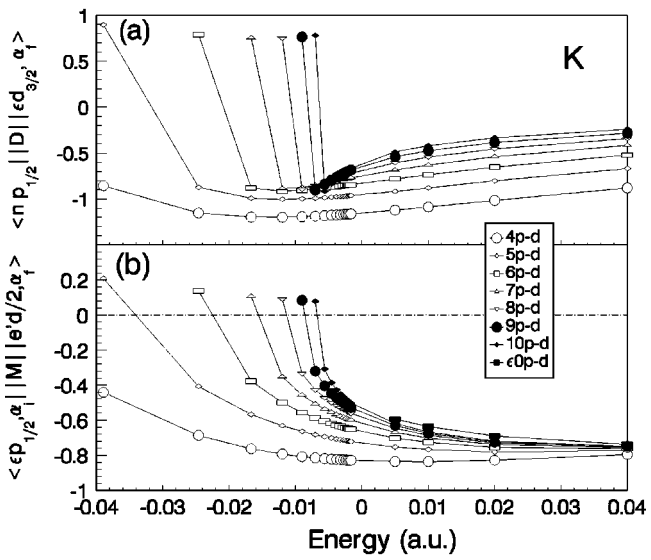

FIG. 3. (a) Final-energy normalized matrix elements $\langle np_{1/2}||D||\epsilon d_{3/2},\alpha_f\rangle$, (b) renormalized matrix elements $\langle \epsilon p_{1/2},\alpha_i||M||\epsilon' d_{3/2},\alpha_f\rangle$ for K, here $\epsilon 0=0.01$ a.u.

tivistic continuum eigenchannel wave functions. Then we can calculate the matrix elements [28–30] with proper asymptotic correction [31].

First, let us consider the transition processes from channel $s_{1/2}$ to channel $p_{1/2}$. The final-energy normalized transition matrix elements of K and Cs are shown in Fig. 1(a) and Fig. 2(a), respectively. Each curve represents the transition from a specific initial state $ns_{1/2}$ to a final channel $p_{1/2}$ and varies smoothly with the final energy across the ionization threshold. The renormalized transition matrix elements from the initial channel $s_{1/2}$ to the final channel $p_{1/2}$ are shown in Fig. 1(b) and Fig. 2(b) for K and Cs, respectively. The curve labeled ''$\epsilon 0s$-p'' represents the transitions from an initial continuum state ($\epsilon 0=0.01$ a.u.). All the curves form a smooth surface, as shown in Fig. 1(b) and Fig. 2(b). Note that in Fig. 1(a) and Fig. 2(a) the starting point of each curve shows a singular behavior as the initial energy $\epsilon_i\rightarrow 0$ (i.e., $n_i\rightarrow\infty$), and however, there is a smooth variation for the renormalized transition matrix element as shown in Fig. 1(b) and Fig. 2(b). With only a few benchmark points on the surface, we can obtain the renormalized transition matrix elements by interpolation. It should provide a compact presentation of the infinitely many transitions to avoid the formidable task of tabulating the transition arrays as shown above in the discussion of the accuracy of our calculated results. It can also be a useful way to check systematically the intrinsic consistency of the ''infinitely many'' transition arrays. For the transition processes ''$p_{1/2}$-$d_{3/2}$'' and ''$d_{3/2}$-$f_{5/2}$,'' there

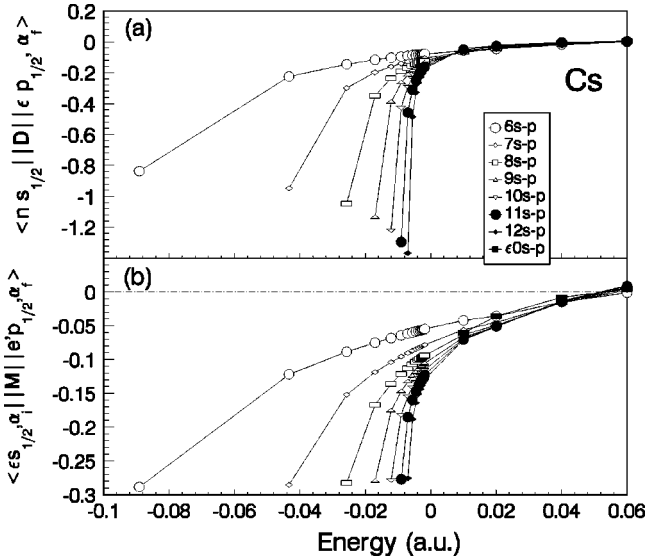

FIG. 2. (a) Final-energy normalized matrix elements $\langle ns_{1/2}||D||\epsilon p_{1/2},\alpha_f\rangle$, (b) renormalized matrix elements $\langle \epsilon s_{1/2},\alpha_i||M||\epsilon' p_{1/2},\alpha_f\rangle$ for Cs, here $\epsilon 0=0.01$ a.u.

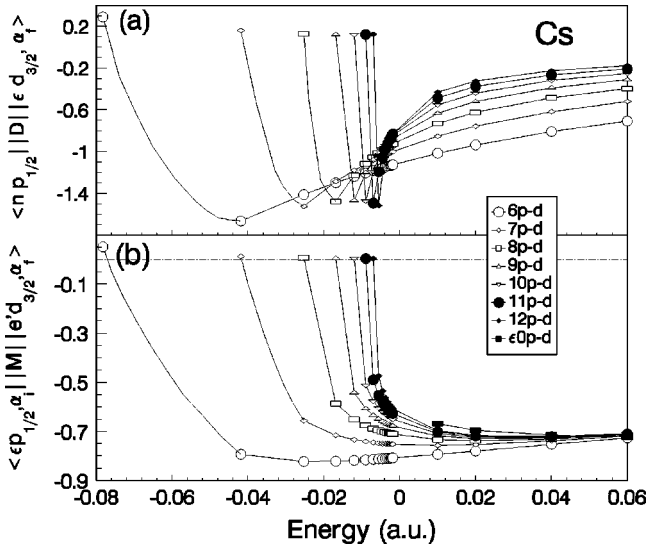

FIG. 4. (a) Final-energy normalized matrix elements $\langle np_{1/2}||D||\epsilon d_{3/2},\alpha_f\rangle$, (b) renormalized matrix elements $\langle \epsilon p_{1/2},\alpha_i||M||\epsilon' d_{3/2},\alpha_f\rangle$ for Cs, here $\epsilon 0=0.01$ a.u.

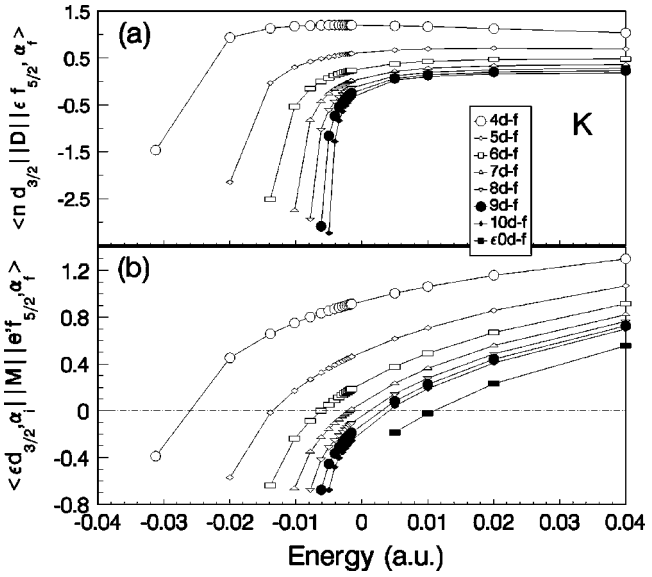

FIG. 5. (a) Final-energy normalized matrix elements $\langle nd_{3/2}||D||\epsilon f_{5/2},\alpha_f\rangle$, (b) renormalized matrix elements $\langle \epsilon d_{3/2},\alpha_i||M||\epsilon' f_{5/2},\alpha_f\rangle$ for K, here $\epsilon 0 = 0.01$ a.u.

exist similar properties, as shown in Fig. 3 and Fig. 5 for K, and Fig. 4 and Fig. 6 for Cs.

III. DISCUSSION

We have defined the renormalized transition matrix elements from initial eigenchannels to final eigenchannels in expression (5). The MQDT parameters $(\mu_\alpha, U_{i\alpha})$ and the eigenchannel wave functions $|\alpha_i\rangle$ and $|\alpha_f\rangle$ can be calculated by relativistic multichannel theory [17–20]. Then the renormalized transition matrix elements $\langle\alpha_i||M||\alpha_f\rangle$ for benchmark points can be calculated and any renormalized transition matrix elements can be obtained conveniently by interpolation. The mixing coefficients $A^{\epsilon_i}_{\alpha_i}$ for initial-energy eigenstate and mixing coefficients $A^{\epsilon_f}_{\alpha_f}$ for final-energy eigenstate can be calculated analytically through MQDT parameters $(\mu_\alpha, U_{i\alpha})_i$ and $(\mu_\alpha, U_{i\alpha})_f$, respectively [9–15]. Thus we can get any transition matrix element and the corresponding oscillator strength (or oscillator strength density) and cross section according to the expressions (4)–(9).

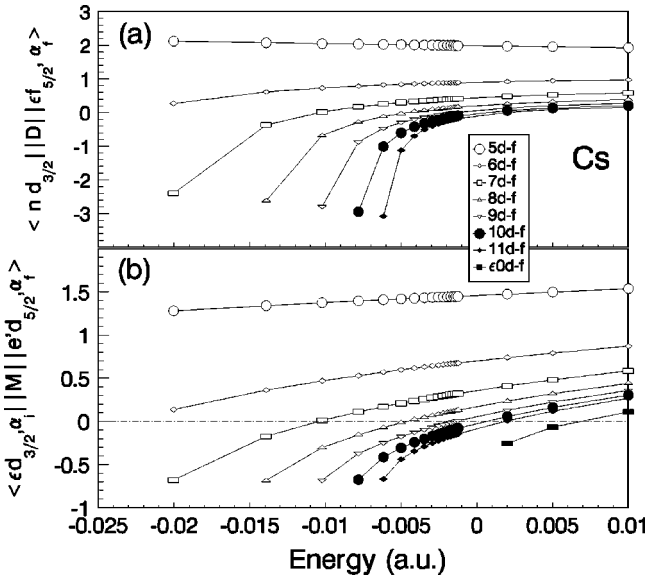

FIG. 6. (a) Final-energy normalized matrix elements $\langle nd_{3/2}||D||\epsilon f_{5/2},\alpha_f\rangle$, (b) renormalized matrix elements $\langle \epsilon d_{3/2},\alpha_i||M||\epsilon' f_{5/2},\alpha_f\rangle$ for Cs, here $\epsilon 0 = 0.01$ a.u.

As mentioned before, all the transition processes from infinitely many states in an initial eigenchannel to infinitely many states in a final eigenchannel can be treated as transitions between a certain pair of initial and final eigenchannels, and then, the state-to-state calculations, which may seem formidable at first glance, can be greatly simplified. Furthermore, the transitions from initial eigenchannels to final eigenchannels can be classified into two categories: (1) transitions between certain pairs of eigenchannels involving only large l, and (2) transitions between certain pairs of eigenchannels involving small l. They should be calculated separately.

For the first category, both the initial and final eigenchannels involving large l are nonpenetrating eigenchannels with quantum defect $\mu \approx 0$ because of the centrifugal potential. They are reduced to one-channel problems, respectively. Therefore, the eigenchannel wave functions can be described exactly as hydrogenic wave functions. Although the number of pairs of channels involving only large l is huge, the renormalized transition matrix elements can be calculated analytically [32]. The earlier works by Bates and Damgaard, Burgess, Seaton, and Peach [3–6] should also be applicable. For the second category (in general, it is a multichannel problem because the penetrating channels with small l are involved), the renormalized transition matrix elements cannot be calculated by analytical hydrogenic formulas. In this case, the difference of quantum defect between initial and final states does not equal zero. For a certain initial state ϵ_i, the final-energy normalized transition matrix element has nodes, at which the matrix element is equal to zero [33]. When we consider all the states ϵ_i in an initial channel, there exist nodal curves on the surface of the renormalized transition matrix element. For example, consider the transitions from the channel $d_{3/2}$ to the channel $f_{5/2}$ for K, as shown in Fig. 5 (the nodal curve is denoted as the dot-dashed line). The difference of quantum defect $\Delta\mu_{nd} = \mu_{\infty f} - \mu_{nd}$ is an important parameter to describe the position of the final energy of the nodes [33]. Since $\Delta\mu_{4d} > \Delta\mu_{5d} > \Delta\mu_{6d} > \Delta\mu_{7d} > -0.41 > \Delta\mu_{8d} > \cdots > \Delta\mu_{\infty d} \simeq 0.001 - 0.56 = -0.559$, the final-energy positions of the nodes for transitions from the initial states, $4d$, $5d$, $6d$, and $7d$, are negative and the final-energy positions of the nodes for transitions from the initial states, $8d$, $9d$, ..., ∞d, are positive. Such matrix elements near the nodal curves cannot be calculated analytically, since the main contributions are coming from smaller radial distances. The renormalized transition matrix elements here are calculated in an exact numerical manner without any analytical approximations. Since the number of pairs of channels involving small l for dipole allowed transitions is limited (restricted by the dipole selection rules), these transitions can be calculated and compiled through a limited number of surfaces, as shown in part (b) of Figs. 1–6 for K and Cs. With only a few benchmark points on the surfaces, the transitions from any states in the initial channel to any states in the final channel can be obtained conveniently by interpolation.

ACKNOWLEDGMENTS

This work was partially supported by the Chinese Science and Technology Commission, National High-Tech ICF Committee in China, Science and Technology Funds of CAEP, Chinese Research Association for Atomic and Molecular Data and the Chinese NSF. The authors would like to express their thanks to Professor A. F. Starace for his helpful comments.

[1] E.g., W. L. Wiese, M. W. Smith, and B. M. Glennon, *Atomic Transition Probabilities*, Natl. Bur. Stand. (U.S.) Circ. No. NSRDS-NSBS 35 (U.S. GPO, Washington, DC, 1966); Oak Ridge National Laboratory Report No. ORNL-6098, 1985 (unpublished); Oak Ridge National Laboratory Report No. ORNL-6551, 1989 (unpublished).

[2] E. W. Thomas, R. K. Janev, and J. J. Smith, International Atomic Energy Agency Report No. INDC(NDS)-249, 1992 (unpublished).

[3] D. R. Bates and A. Damgaard, Philos. Trans. R. Soc. London, **242**, 101 (1949).

[4] A. Burgess and M. J. Seaton, Mon. Not. R. Astron. Soc. **120**, 121 (1960).

[5] G. Peach, Mem. R. Astron. Soc. **71**, 13 (1967).

[6] G. Peach, Mon. Not. R. Astron. Soc. **130**, 361 (1965).

[7] M. J. Seaton, Proc. Phys. Soc. London **88**, 801 (1966); Rep. Prog. Phys. **46**, 167 (1983).

[8] U. Fano, Phys. Rev. A **2**, 353 (1970).

[9] U. Fano, J. Opt. Soc. Am. **65**, 979 (1975).

[10] C. Greene, U. Fano, and G. Strinati, Phys. Rev. A **19**, 1485 (1979).

[11] C. M. Lee (Jia-Ming Li) and K. T. Lu, Phys. Rev. A **8**, 1241 (1973).

[12] C. M. Lee (Jia-Ming Li), Phys. Rev. A **10**, 584 (1974).

[13] C. M. Lee (Jia-Ming Li) and W. R. Johnson, Phys. Rev. A **22**, 975 (1980).

[14] J. M. Li, Acta Phys. Sin. **29**, 419 (1980).

[15] J. M. Li, Acta Phys. Sin. **32**, 84 (1983).

[16] L. Liu and J. M. Li, Acta Phys. Sin. **42**, 1901 (1993).

[17] W. Huang, Y. Zou, X. M. Tong, and J. M. Li, Phys. Rev. A **52**, 2770 (1995).

[18] Y. Zou, X. M. Tong, and J. M. Li, Acta Phys. Sin. **44**, 50 (1995).

[19] X. M. Tong, Y. Zou, and J. M. Li, Chin. Phys. Lett. **12**, 351 (1995).

[20] Y. Zou, X. M. Tong, and J. M. Li, Chin. Phys. Lett. **13**, 269 (1996).

[21] N. B. Delone, S. P. Goreslavsky, and V. P. Krainov, J. Phys. B **22**, 2941 (1989); **27**, 4403 (1994).

[22] U. Fano and J. W. Cooper, Rev. Mod. Phys. **40**, 441 (1968).

[23] D. A. Liberman, D. T. Comer, and J. T. Waber, Comput. Phys. Commun. **2**, 107 (1971).

[24] J. M. Li and Z. X. Zhao, Acta Phys. Sin. **31**, 97 (1982).

[25] Jun Yan, Pei-Hong Zhang, Xiao-Min Tong, and Jia-Ming Li, Acta Phys. Sin. **45**, 1978 (1996).

[26] W. L. Wiese, M. W. Smith, and B. M. Glennon *Atomic Transition Probabilities*, Natl. Bur. Stand. (U.S.) Circ. No. NSRDS-NSBD 4 (U.S. GPO, Washington, DC, 1969).

[27] C. E. Moore, J. Phys. B **14**, 9 (1981).

[28] I. P. Grant, Comput. Phys. Commun. **4**, 263 (1973).

[29] Z. X. Zhao and J. M. Li, Acta Phys. Sin. **34**, 1469 (1985).

[30] C. M. Lee, Lynn Kissel, and R. H. Pratt, Phys. Rev. A **13**, 1714 (1976).

[31] E. R. Smith, J. Comput. Phys. **18**, 201 (1975).

[32] H. A. Bethe and E. E. Salpeter, *Quantum Mechanics of One- and Two-Electron Atoms* (Springer, Berlin, 1957); L. J. Slater, *Confluent Hypergeometric Functions* (Cambridge University Press, Cambridge, 1960).

[33] E.g., X. L. Liang and J. M. Li, Acta Phys. Sin. **34**, 1479 (1985); M. S. Wang and R. H. Pratt, Phys. Rev. A **29**, 174 (1984); R. Y. Yin and R. H. Pratt, *ibid.* **35**, 1154 (1987); X. M. Tong, L. Yang, and J. M. Li, Acta Phys. Sin. **38**, 407 (1989).

[34] C. E. Moore, *Atomic Energy Levels*, Natl. Bur. Stand. (U.S.) Circ. No. NSRDS-NBS 35 (U.S. GPO, Washington, DC, 1971).